Cell Reports
Physical Science

CellPress
OPEN ACCESS

Article

Switching between intramolecular charge transfer and excimer emissions in solids based on aryl-modified ethynyl–*o*-carboranes

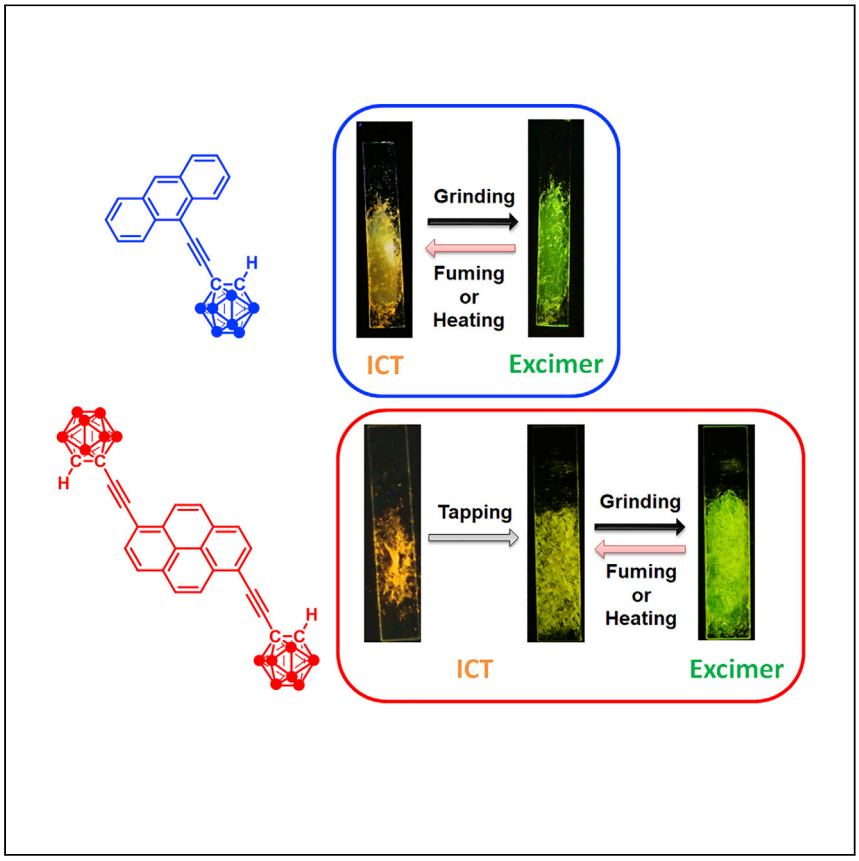

Yamamoto et al. synthesize solid-state stimulus-responsive luminescent *o*-carboranes. Switching between different luminescent mechanisms by mechanical forces is demonstrated, and multi-step mechanochromic luminescence to weak stimuli is accomplished.

Hideki Yamamoto, Junki Ochi, Kazuhiro Yuhara, Kazuo Tanaka, Yoshiki Chujo

tanaka@poly.synchem.kyoto-u.ac.jp

Highlights

Solid-state luminescent *o*-carboranes are presented

Unique stimulus responsiveness is demonstrated

Switching between different luminescent mechanisms is demonstrated

Multi-step mechanochromic luminescence is accomplished

Yamamoto et al., Cell Reports Physical Science 3, 100758
February 16, 2022
https://doi.org/10.1016/j.xcrp.2022.100758

Cell Reports
Physical Science

CellPress
OPEN ACCESS

Article

Switching between intramolecular charge transfer and excimer emissions in solids based on aryl-modified ethynyl–*o*-carboranes

Hideki Yamamoto,[1] Junki Ochi,[1] Kazuhiro Yuhara,[1] Kazuo Tanaka,[1,2,*] and Yoshiki Chujo[1]

SUMMARY

Because of its unique electronic properties, *o*-carborane has attracted attention as a scaffold for constructing solid-state luminescent materials. Here, we report stimulus-responsive luminochromic materials based on polycyclic aromatic hydrocarbon (PAH), such as anthracene and pyrene, modified with the ethynyl-*o*-carborane unit. Initially, luminochromism originating from switching of different emission mechanisms is described between intramolecular charge transfer (ICT) emission and excimer emission triggered by mechanical stimuli, heat, and vapor annealing regarding the single *o*-carborane-substituted anthracene. Next, the luminescence properties of two ethynyl-*o*-carboranes at both ends of PAHs are presented. In particular, multi-step mechanochromic luminescence of the pyrene derivative is explained. Stepwisely changes triggered by weak stimuli that can induce cracking sites, followed by luminochromic behavior and by grinding treatment, which causes phase transition from crystal to amorphous, leading to luminescent mechanism changes from ICT emission to excimer emission.

INTRODUCTION

o-Carborane is an icosahedral cluster composed of 10 boron and two carbon atoms.[1–5] Because of its unique electronic properties, such as a strong electron-accepting ability when bonded at the carbon atom, *o*-carborane has attracted attention as a scaffold for constructing solid-state luminescent materials. In particular, from the findings of aggregation-induced emission (AIE) from *o*-carborane-containing polymers, various unique luminescence behaviors, such as AIE, crystallization-induced emission, and stimulus-responsive luminochromism, have been discovered in the conjugated molecules, involving *o*-carborane-aromatic rings.[6–12] Advanced optical materials with circular polarized luminescence[13,14] and laser amplification properties[15] were obtained based on *o*-carborane derivatives. One significant photochemical character is switching of the excitation states between locally excited (LE) and intramolecular charge transfer (ICT) states by intramolecular rotation in the polycyclic aromatic hydrocarbon (PAH)-modified *o*-carboranes (Figure S11).[16–18] When the angle of the C-C bond to the π plane is parallel (0°), electronic conjugation is minimized between the aryl moiety and the *o*-carborane unit.[19] Therefore, very weak LE emission from the aryl moiety is observed in solids because of critical concentration quenching. In contrast, ICT emission can be observed from the perpendicular conformation between the C-C bond to the π plane. The *o*-carborane unit can rotate in the excited state in crystals, followed by solid-state luminescence with the ICT character.[13,20,21] For example, anthracene-tethered *o*-carborane (**CBA**; Figure 1) has AIE with the ICT character, and the high solid-state emission

[1]Department of Polymer Chemistry, Graduate School of Engineering, Kyoto University Katsura, Nishikyo-ku, Kyoto 615-8510, Japan

[2]Lead contact

*Correspondence: tanaka@poly.synchem.kyoto-u.ac.jp

https://doi.org/10.1016/j.xcrp.2022.100758

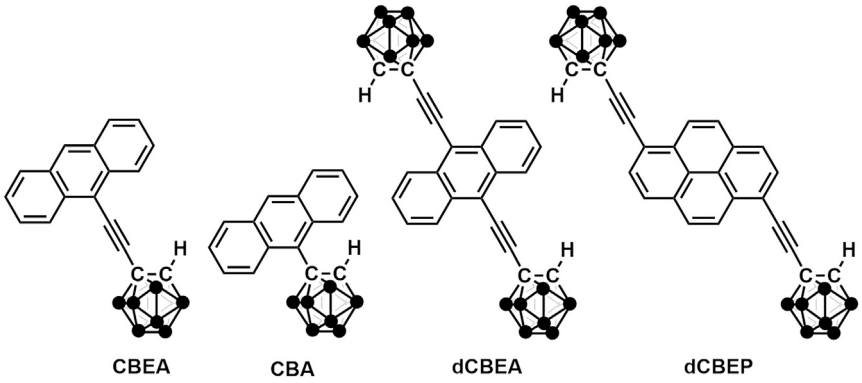

Figure 1. Chemical structures of *o*-carborane derivatives used in this study

efficiency depended on the type of substituents (R in Figure S11).[20] In the case of methyl and trimethylsilyl groups, almost quantitative emission efficiencies were detected. Moreover, by suppressing rotation by introducing a bulky substituent at the adjacent carbon, almost quantitative solid-state emission yields were obtained.[20] It has been demonstrated that thermochromic luminescent properties in crystals can be controlled by regulating the energy barrier in the rotation of the *o*-carborane unit with the substituents around *o*-carborane units.[22,23] Thus, PAH-*o*-carborane is a promising platform for designing not only solid-state luminophores but also stimulus-responsive materials. Especially mechanochromic luminescent materials presenting irreversible changes by mechanical forces can be used as a stress memory without a battery or wiring. If the materials can detect weak mechanical forces, then highly sensitive detection would be expected.

We have proposed the concept of designing functional materials based on an "element block," which is a minimum functional unit containing heteroatoms.[24–27] Based on this idea, various types of solid-state luminescence and stimulus-responsive luminochromic behaviors were accomplished by *o*-carborane-modified, π-conjugated molecules.[28–37] Since the discovery of the solid-state excimer of the *o*-carborane derivative,[38] we also found that the PAH-ethynyl-*o*-carborane structure is an element block for expressing excimer emission in the solid state.[39,40] By combination with PAHs, unique luminescence properties were discovered. For example, acridine-modified ethynyl-*o*-carboranes were synthesized, and solid-state excimer emission was observed.[39,40] In the crystal packing, dimer structures assisted by the hydrogen bond between nitrogen in acridine and hydrogen in *o*-carborane were formed. It has been suggested that the degree of π-π interaction between one of the acridines in the dimer and the next acridine in another dimer could be responsible for the color of the excimer emission. In particular, because of environmental sensitivity of the π-π interaction, thermochromic luminescence properties of excimer emission were also observed. As another example, from the crystal of pyrene-modified ethynyl-*o*-carborane, the switching behaviors of luminescence mechanisms between ICT and excimer emissions were observed.[41] Under ambient temperature, the typical ICT emission was observed from a crystal powder, whereas excimer emission appeared by cooling at 77 K. As a result, clear thermochromic luminescence between orange and green was obtained. Moreover, because pyrene-modified ethynyl-*o*-carborane slowly exhibits aggregation in organic solvents, followed by aggregation-induced excimer emission, detection of water content in organic solvents was accomplished.[42] Because of these results, we think that PAH-ethynyl-*o*-carborane is an element block for designing a stimulus-responsive luminochromic material having solid-state excimer emission

properties. Especially, we presume that advanced environmental sensors could be produced by applying high-sensitivity of excimer emissions to environmental changes.

Here we report a solid-state excimer emission and its environmental sensitivity from anthracene- and pyrene-modified ethynyl-*o*-carboranes. Initially, we explain optical properties of mono-substituted ethynyl-*o*-carborane with anthracene. Accordingly, the luminochromic behavior caused by switching photochemical processes between excimer emission and ICT one by external stimuli, such as physical forces and heating, was demonstrated. Next, the molecular design to realize stimulus-responsive luminochromism originating from emission mechanism changes with much tender stimuli is illustrated. The optical properties of bis-substituted *o*-carboranes with anthracene[43] and pyrene are described. Yellow and green luminescent samples of the anthracene triad exhibiting almost the same X-ray diffraction patterns are shown. A plausible model is proposed, showing that the degree of defect sites might be responsible for the luminescence color. In particular, multi-step mechanochromic luminescence from pyrene-substituted ethynyl-*o*-carborane is demonstrated by gently touching the crystalline sample and subsequently grinding them. Using X-ray structure analyses, we discuss the mechanism of luminochromic behavior concerning solid-state excimer emission and sensitive responsiveness by focusing on the sparse packing induced by the ethynyl-*o*-carborane unit. In this study, we show that the ethynyl-*o*-carborane unit also plays a role in stimulus-responsive luminescent materials based on the luminescent mechanism shifts in the solid state.

RESULTS AND DISCUSSION

Synthesis and characterization

The syntheses are illustrated in the Experimental procedures, and the characterization data are shown in the supplemental information. Figure 1 shows the modified ethynyl-*o*-carboranes used in this study. 1-Ethynyl-*o*-carborane was synthesized according to the literature,[39,40] and the Sonogashira-Hagihara cross-coupling reaction with 9-iodoanthracene afforded 9-((1-*o*-carboranyl)ethynyl)anthracene (**CBEA**) (Figure S12). By using 9,10-diiodoanthracene as a starting material, the bis-substituted compounds 9,10-bis((1-*o*-carboranyl)ethynyl)anthracene (**dCBEA**)[43] and 1,6-bis((1-*o*-carboranyl)ethynyl)pyrene (**dCBEP**) were prepared with ethynyl-anthracene and -pyrene derivatives, respectively. The structures of the products were characterized by NMR spectroscopy and high-resolution mass spectroscopy (Figures S1–S9). All carboranes show good solubility in organic solvents such as dichloromethane, chloroform, and tetrahydrofuran and stability under ambient conditions and light irradiation.

The single-substituted anthracene derivative CBEA

Figure 2A shows the UV-visible (UV-vis) absorption and photoluminescence (PL) spectra of **CBEA** in tetrahydrofuran (THF) (1.0×10^{-5} M). In the UV-vis absorption spectrum, the vibrational structure was detected around 400 nm, assigned to the π–π^* transition band of the anthracene moiety. In the PL spectrum, only LE emission with vibrational peaks around 450 nm was observed. It is likely that ICT emission was quenched by the vibrational motion at the C-C bond of the *o*-carborane moiety. In contrast, as shown in the PL spectra in solids in Figure 2B, only ICT emission around 590 nm was observed in the crystalline state. This property was similar to that of **CBA** in the solid state. The emission color was changed from orange to green, with a wavelength shift up to 50 nm after grinding the crystal with a stainless steel spoon, indicating that **CBEA** has mechanochromic luminescence properties (Figure 2B).

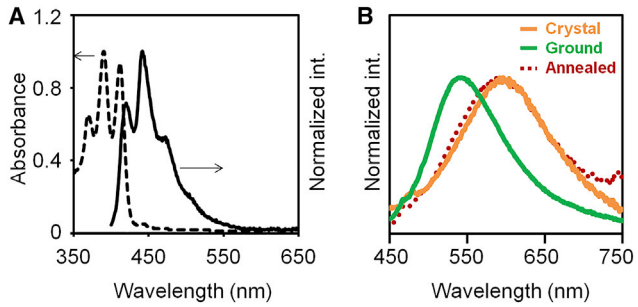

Figure 2. Optical properties of CBEA

(A) UV-vis absorption and PL spectra in THF (1.0×10^{-5} M).

(B) PL spectra of the crystal, ground and annealed after grinding samples

To investigate the origin of the emission peak around 540 nm generated by grinding, the concentration-dependent PL spectra of **CBEA** were initially examined in THF solution and H_2O/THF mixtures (Figure S13). A new emission peak, which was similar to that of the ground sample, appeared when the ratio of H_2O/THF mixtures was over 90%. Furthermore, the lifetime (13.7 ns) of an H_2O/THF mixture of 99% was almost the same as a new lifetime component of the ground crystal (12.5 ns) (Table 1). Thus, the emission band around 540 nm was strongly suggested to be excimer emission.

We obtained single crystals of **CBEA** large enough for applying X-ray crystallography. Therefore, to determine why the excimer emission was observed by introducing an ethynyl spacer between anthracene and *o*-carborane, we compared the single-crystal structures of **CBEA** and **CBA**, which provides solid-state emission from the ICT state (Figure 3).[13,20] According to the structural data, there are several significant points. First, π-π interactions between the adjacent anthracene planes were compared.[39,40] In the case of **CBA**, the anthracene plane was distorted, and the distance between them was quite long (7.904 Å). It is likely that the bulky *o*-carborane contributes to isolate each molecule. On the other hand, the anthracene planes of **CBEA** show high planarity, and the distance (3.414 Å) was much shorter than that of **CBA**. This suggests that a rigid ethynyl spacer mitigates intra- and intermolecular interactions. Therefore, excimer formation can be occasionally detected through the intermolecular interaction in the ethynyl-spacer-containing *o*-carboranes.[41,42] Next, we compared the unit cells of **CBA** and **CBEA**. We found that the density and the packing ratio of **CBEA** are smaller than those of **CBA** (Table S1). This indicates that introducing an ethynyl spacer leads to a less dense molecular arrangement.

Zhang et al.[44] studied anthracene-arrangement-dependent emissions of crystals of 9-anthrylpyrazole derivatives and provided new insights into the relation between chromophore arrangement and emission behavior. This suggests that the emission colors of crystals are strictly related to the intermolecular packing degree of the anthracene moieties. If more than two-thirds of an anthracene ring participates in the overlap, the emission color should be altered from blue to green. In the case of **CBEA**, the overlapping area is about 38% (Figure S10). This value is obviously small, meaning that a weak π-π interaction at the anthracene moieties would be formed. From these data, we propose the emission mechanism of **CBEA**. In the crystal state, ICT emission is favorable because of the ordered and less molecular arrangement. After grinding, the crystal structure collapses, and the overlapping area is magnified. Then strong π-π interaction could be favorable for excimer

Table 1. Optical properties of CBEA

condition	λ_{PL} (nm)	τ (ns)[a]	Φ_{PL}[b]
THF	442[c]	5.15 (100%)	<0.01
Crystal	592[d]	35.0 (100%)	0.01
Ground	543[d]	12.5 (30%) 37.6 (70%)	<0.01
H_2O (99%)	545[e]	3.00 (21%) 13.7 (79%)	<0.01

[a]We calculated the decay curve with the excitation light at 375 nm, as shown in Figure S11.
[b]Determined as an absolute value with an integration sphere.
[c]Excited at 390 nm.
[d]Excited at λ_{abs} in THF (1×10^{-5}M).
[e]Excited at 397 nm.

emission. It is suggested that different mechanisms of ICT emission and excimer emission could be switched by external stimuli when an ethynyl spacer is introduced between anthracene and *o*-carborane.

When the ground crystal was annealed by heat or a solvent vapor, like $CHCl_3$, the emission color returned to orange (Figure 4A). These grinding and annealing processes were repeated at least 5 times (Figure 4B). To examine the mechanism of reversibility, we performed powder X-ray diffraction (PXRD) with **CBEA** (Figure S14). The pattern of the crystal state exhibited sharp peaks, whereas the pattern was hardly observed after grinding. Then the peaks appeared again after annealing the ground crystal. These results indicate that the crystal state of **CBEA** became the amorphous state after grinding and induced the change of the emission mechanism from ICT emission to excimer emission.

We carried out differential scanning calorimetry (DSC) analysis with **CBEA** (Figure S15). Significant peaks were not observed below 250°C, where pyrolysis occurs. On the other hand, the ground crystal showed an exothermic peak at around 120°C. An emission color change from green to orange can be observed at around this temperature by heating the ground crystal, supporting the speculation that the phase transition should proceed from amorphous to crystal.

The dual-substituted anthracene derivative dCBEA

From the solid-state emission from the excimer state and stimulus-responsive luminochromic behavior, we designed bis-*o*-carborane-substituted molecules for realizing sensitive behavior toward much tiny environmental changes. To evaluate the validity of this idea, we synthesized the anthracene- and pyrene-substituted compounds **dCBEA** and **dCBEP**, respectively (Figure 1). We prepared both compounds using Sonogashira-Hagihara cross-coupling reactions. The products were characterized with NMR spectroscopy and mass measurements. According to the characterization data, the desired compounds were obtained.

Figure 5A shows the UV-vis absorption and PL spectra of **dCBEA** in THF (1.0×10^{-5} M). It is known that **dCBEA** is an AIE-active molecule.[43] In our study, the π-π^* transition band of the anthracene moiety in the absorption spectrum and LE emission in the PL spectrum were observed, similarly to **CBEA**. Interestingly, when **dCBEA** was crystallized from the same solvent (mixtures of $CHCl_3$ and MeOH), two different types of luminescent crystals exhibiting a green or yellow color were afforded (G form and Y form). When **dCBEA** was crystallized rapidly at room temperature, the major crystal color was green, and when crystallized slowly at −50°C, a

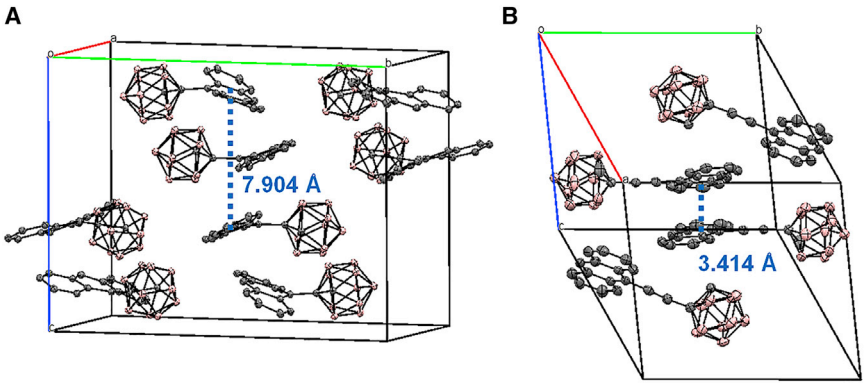

Figure 3. Single crystal X-ray data of anthracene-tethered *o*-carboranes
(A) Crystal packing of **CBA**.
(B) Crystal packing of **CBEA**.

yellow-emitting crystal was easily obtained. Figure 5B shows the PL spectra of the two crystals. The emission band of the G-form crystal has a vibrational structure. Iida and Yamaguchi[45] reported that intense LE emission from the anthracene moiety in the solid state is inducible by introducing (pentafluorophenyl)dimethylsilyl groups to a 9,10-diphenylanthracene skeleton as the π-stacking tethers. Furthermore, Fujiwara et al.[46] reported that dual alkylene-strapped 9,10-diphenylanthracene derivatives also exhibit intense LE emission in the solid state because of inhibition of the anthracene moiety from non-specific intermolecular interactions by the substituents. The anthracene skeleton of **dCBEA** was also isolated from the interaction because of steric hindrance of bulky ethynyl-*o*-carborane. Indeed, the lifetime component and quantum yield in the G form (τ = 0.64 ns, Φ_{PL} = 0.04) were similar to those in THF (τ = 1.00 ns, Φ_{PL} = 0.03) (Table S2). Therefore, emission of the G form is attributable to LE emission. On the other hand, the emission of the Y form could be ICT emission because of its long lifetime. In terms of ICT emission, **CBEA** showed weak emission, and its quantum yield was 0.01, whereas the Y form of **dCBEA** showed strong emission, and its quantum yield increased to 0.12. By gradually growing the Y-form crystal, most *o*-carboranes should be regularly and tightly aligned. Thus, intense ICT emission might be induced.

To address the relationship between the emission mechanism and the molecular conformation, density functional theory (DFT) and time-dependent DFT (TD-DFT) were performed (Figure S16). In the planar conformation (the dihedral angles are 0 and 180°), the highest occupied molecular orbital (HOMO) and lowest unoccupied molecular orbital (LUMO) were centered on the anthracene unit. These results mean that the π-π* transition of the anthracene moiety and, subsequently, LE emission should proceed in the planar conformation. In contrast, in the twisted conformation (the dihedral angles are 90° and 270°), the LUMO extended to the C-C bond in the *o*-carborane unit, meaning that σ*-π* transition from anthracene to *o*-carborane followed by ICT emission should be possible. These data corresponded to those of series of PAH-*o*-carborane dyads in previous reports.[16–18]

To investigate the mechanism of different crystalline forms of the same substance, we compared G-form and Y-form crystals of **dCBEA** using various methods. Predictably, exactly the same ^{1}H NMR spectra were obtained from the solution, meaning that hardly any degradation and isomerization occurred (Figure S17). Furthermore, the solvents for recrystallization ($CHCl_3$ and MeOH) had no effect on their optical

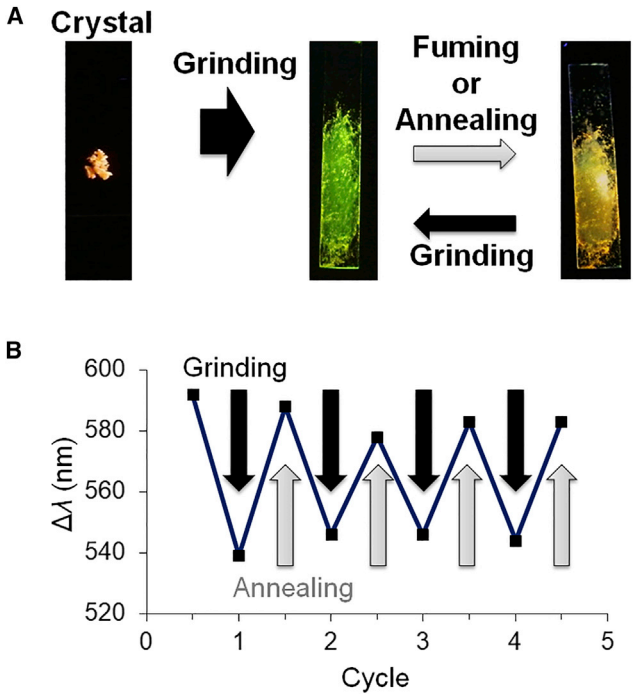

Figure 4. Luminochromic behavior of CBEA

(A) Solid-state luminescent chromism toward various stimuli. Pictures were taken under UV irradiation (365 nm).

(B) Reversibility in the grinding and annealing cycles.

properties. Surprisingly, single-crystal structures or polycrystalline structures were also identical (Figures S18 and S19; Tables S3 and S4). Therefore, the difference between their emission spectra should not be from crystal packing or polymorphism.

Scanning electron microscopy (SEM) measurements of the G form and Y form were carried out (Figure S20). It was revealed that the crystals were different in terms of crystal shape and size. The crystals of the G form were basically thick and large with length of 5–20 μm, whereas those of the Y form were thin and small with a length of 1–5 μm. When single-crystal X-ray diffraction measurements were carried out, we found that the single crystal of the Y form was more vulnerable than that of the G form. Percino et al.[47] reported similar optical and structural properties. They synthesized two crystals of (2Z)-2-(4-bromophenyl)-3-[4-(dimethylamino)phenyl]prop-2-enenitrile and found that their emission colors were different but their crystal structures were identical. This means that crystal shape and size can significantly affect their emission behavior. In our study, taking into account the almost identical XRD patterns of the G form and Y form and the fact that mechanochromic luminescent behavior was hardly observed in **dCBEA**, we suggest that many more defect sites should be generated in the Y form through relatively rapid crystal formation. The number of molecules that are out of regular crystalline packing should be different, followed by a different luminescence color.

The dual-substituted pyrene derivative dCBEP

Finally, we evaluated the optical properties of **dCBEP**. Similar to the previous compounds, in the UV-vis absorption spectrum in THF (1.0×10^{-5} M), the π-π^* transition band of the pyrene moiety was observed (Figure 6A). In addition, LE emission was detected in the PL spectrum, indicating that *o*-carborane units have hardly any

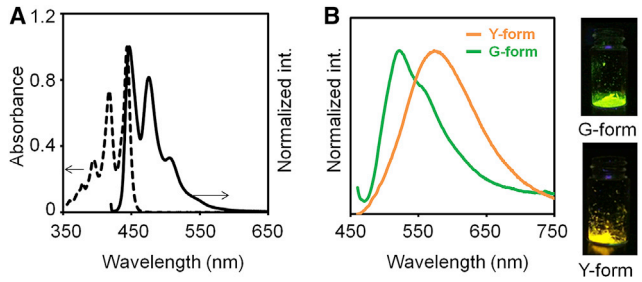

Figure 5. Optical properties of dCBEA

(A) UV-vis absorption and PL spectra in THF (1.0×10^{-5} M).

(B) PL spectra of the crystals.

influence on electronic properties in solution because of molecular rotation. Using analyses with crystalline samples, it was demonstrated that **dCBEP** also afforded two different types of luminescent crystals exhibiting orange and yellow colors (O form and Y form) by different crystallization methods (Figure 6B). The O form was obtained by dissolution in toluene at 110°C and then slow cooling to −30°C. The Y form was prepared by dissolution in a good solvent like THF and then evaporation. It is assumed that the O form is a thermodynamically stable crystal and that the Y form contains more cracking sites. The shapes of their spectra and their lifetime components were almost identical (Table 2). This suggests that both of their emissions are ICT emissions.

Surprisingly, it was revealed that the O form had an extremely rare two-step mechanochromic property depending on different mechanical stimuli (Video S1).[48–51] When the pristine crystal was gently tapped with a stainless steel spoon or pressed with a flat plate, the emission color changed from orange to yellow. Furthermore, when the tapped crystal was ground with a stainless steel spoon, the yellow emission again changed to green (Figure 7). The optical properties of the tapped O-form crystal were very similar to those of the Y-form crystal. In the case of **dCBEP**, cracking sites might be able to be generated by weak stimuli. Therefore, sensitive mechanochromic luminescence could be obtained. A new major lifetime component (15.0 ns) that was longer than the others was observed in the ground O-form crystal (Figure S23; Table 3). This suggests that the green emission can be attributed to excimer emission. This green color changed back to yellow after annealing (heating at 120°C or fuming with toluene vapor), but a further color change was not observed. On the other hand, it was found that the Y-form crystal had similar optical properties, meaning that the luminochromism reversibly proceeds between yellow and green by grinding and annealing processes.

Figure S21 shows the PXRD patterns of the O-form pristine crystal, the tapped crystal, the ground crystal, the annealed crystal, and the Y-form crystal. For the most part, the peaks of the tapped O-form crystal and Y-form crystal are identical to that of the O-form pristine crystal. These data show that the molecular distribution and structures should be the same in the O-form and Y-form crystals. However, some new peaks (2θ = 15.6 and 25.9°) were observed compared with the peaks of the O-form pristine crystal. These results indicate that the main molecular arrangements might be retained by tapping but that a slight change would occur at some parts. After grinding the O-form crystal, the sharp and intense peaks disappeared, indicating that the conversion from the crystal state of the O-form to the amorphous state should be induced after grinding. Wang et al.[48] also reported a boron diketonate crystal exhibiting two-step mechanochromic property by different mechanical

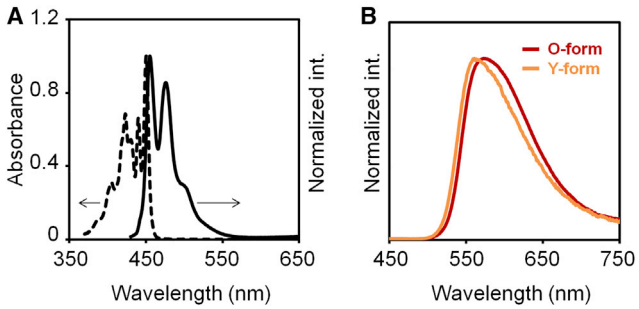

Figure 6. Optical properties of dCBEP

(A) UV-vis absorption and PL spectra in THF (1.0×10^{-5} M).

(B) PL spectra of the crystals.

stimuli. The PXRD pattern of this compound after tapping the pristine crystal showed some new diffraction peaks. They suggested that the new peaks were derived from diffraction of the crack surfaces and that the shift of the emission peak originated from molecular perturbations on the crack surfaces.

To evaluate the sizes of sample powders, SEM observations were performed (Figure S22). Corresponding to the results from **dCBEA**, larger aspect ratios were detected from the crystals in the O form than those of the Y form, meaning that the size of crystal particles could play a significant role in luminescence color. From the ground sample with green luminescence, tiny crashed powders were observed.

From these results, we considered the mechanism of two-step mechanochromic properties of **dCBEP** (Figure 8). After tapping with thermodynamically stable O-form, crystal particles can be readily collapsed by tender forces because of the sparse packing caused by dual *o*-carborane substituents. Consequently, a similar situation could be generated in the Y form, where intermolecular π-π interaction at the pyrene moieties should be extremely weakened. Therefore, orange emission from the ICT state is blue-shifted to yellow. After grinding the fragmental crystal, the phase transition from the crystal state to amorphous proceeds, and the overlap of pyrene moieties can be enhanced in the random distributions. As a result, a strong π-π interaction, which leads to excimer emission, can be formed. Finally, the second color change should be induced. Multiple ethynyl-*o*-carborane units play significant roles in stimulus response as well as solid-state excimer emission.

Here we report functional luminescent materials using *o*-carborane. By introducing an ethynyl spacer between the PAH moiety and *o*-carborane, different emission mechanisms of ICT emission and excimer emission can be switched by external stimuli, such as mechanical stimuli, heat, and vapor annealing. In addition, two different types of luminescent crystals can be observed by substituting ethynyl-*o*-carboranes at both ends of PAHs. Surprisingly, it is revealed that they should be not a polymorph but the same crystal structure from X-ray diffraction measurements. Furthermore, in the case of **dCBEP**, the emission color changes are triggered by tiny mechanical stimuli. It is proposed that making less stable molecular packings by using a steric bulky structure of *o*-carborane and less dense molecular arrangements by introducing an ethynyl spacer might play an important role in these curious optical properties. *o*-Carborane compounds have attracted attention as an element block for designing highly luminescent solid-state materials. In this study, it is demonstrated that the ethynyl-*o*-carborane unit also plays a role in stimulus-responsive luminescent materials based on the luminescent mechanism shifts in the solid state.

Table 2. Optical properties of dCBEP in various states

Condition	λ_{PL} (nm)	τ (ns)[a]	Φ_{PL}[b]
THF	426[c]	2.65	<0.01
O form	575[d]	2.27 (77%)	0.02
		4.13 (23%)	
Y form	561[d]	2.07 (76%)	0.03
		3.81 (24%)	

[a]We calculated the decay curve with the excitation light at 375 nm, as shown in Figure S11.
[b]Determined as an absolute value.
[c]Excited at 373 nm.
[d]Excited at 400 nm.

EXPERIMENTAL PROCEDURES

Resource availability

Lead contact

Further information and requests for resources should be directed to and will be fulfilled by the lead contact, Kazuo Tanaka (tanaka@poly.synchem.kyoto-u.ac.jp).

Materials availability

All materials generated in this study are available from the lead contact.

Data and code availability

The crystallographic information files (CIFs) generated by refinement of all structures in this study, including the original structure factors, have been deposited in the Cambridge Structural Database and can be accessed with deposition numbers CSD: 2112923, 2112924, and 2112925 for **CBEA**, the G form of **dCBEA**, and the Y form of **dCBEA**, respectively. All other data are available from the authors upon request.

General

^{1}H, ^{13}C, and ^{11}B NMR spectra were recorded on a JEOL JNM-EX400 instrument at 400, 100, and 128 MHz, respectively. The ^{1}H and ^{13}C chemical shift values were expressed relative to Me_4Si as an internal standard. The ^{11}B chemical shift values were expressed relative to $BF_3 \cdot Et_2O$ as an external standard (sealed capillary in the case of **dCBEP**). A high-resolution mass spectrum (HRMS) was obtained on a Thermo Fisher Scientific Exactive spectrometer for atmospheric pressure chemical ionization (APCI). The samples were dissolved in appropriate organic solvents and injected into the instrument. Analytical thin-layer chromatography (TLC) was performed with silica gel 60 Merck F254 plates. Column chromatography was performed with Wakogel C-300 silica gel. UV-vis absorption spectra were obtained on a Shimadzu UV3600 spectrophotometer. PL spectra were obtained on a Horiba FluoroMax-4 luminescence spectrometer. Fluorescence quantum yield (QY) was recorded on a Hamamatsu Quantaurus-QY Plus C13534-01 model. PXRD patterns were taken by CuKα radiation with Rigaku Miniflex. In case of **CBEA**, X-ray crystallography analyses were carried out by a Rigaku R-AXIS RAPID-F graphite-monochromated MoKα radiation diffractometer with an imaging plate and a Rigaku XtaLAB PRO graphite-monochromated CuKα radiation diffractometer with an imaging plate in the case of **dCBEA**. DSC thermograms were obtained on an SII DSC 6220 instrument at a heating rate of 10°C/min. SEM was recorded on a JEOL JSM-5600 instrument.

Materials

All synthetic procedures were performed under an Ar atmosphere. THF and triethylamine were purchased and purified by passage through a purification column under Ar pressure. CuI, $Pd_2(dba)_3$, and tri(2-furyl)phosphine (TFP) were obtained

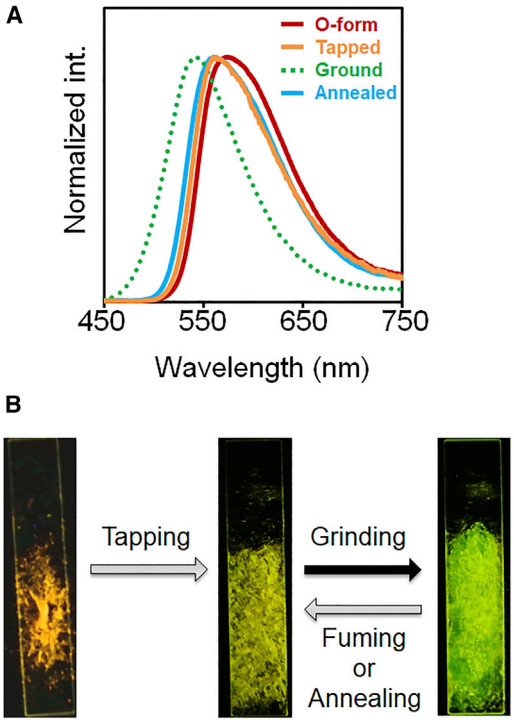

Figure 7. Luminochromic behavior of dCBEP

(A) Solid-state luminescent chromism toward various stimuli.

(B) Pictures were taken under UV irradiation (365 nm).

commercially and used without purification. 1-Ethynyl-*o*-carborane, 9-iodoanthracene, 9,10-diiodoanthracene, and 1,6-diiodopyrene were synthesized and characterized according to the literature.[52–55]

Synthesis of CBEA

A mixture of 1-ethynyl-*o*-carborane (0.1699 g, 1.01 mmol), 1-iodoanthracene (0.3648 g, 1.20 mmol), CuI (0.0381 g, 0.198 mmol), $Pd_2(dba)_3$ (0.0236 g, 0.026 mmol), and TFP (0.0360 g, 0.155 mmol) was dissolved in 5 mL of THF and 5 mL of triethylamine under an Ar atmosphere. The mixture was stirred at 50°C for 18 h and washed with NH_4Cl and brine, and the organic layer was dried over $MgSO_4$. After $MgSO_4$ was removed, the solvent was evaporated. The residue was purified by column chromatography on silica gel (hexane/THF, v/v = 7:1). After evaporation of the solvent, recrystallization from $CHCl_3$/MeOH afforded compound **CBEA** as a yellow solid (0.2100 g, 0.610 mmol, 61%). ^{1}H NMR (400 MHz, $CDCl_3$; Figure S1): 8.50 ppm (1H, s, Ar-*H*), 8.27 ppm (2H, d, *J* = 8.80 Hz, Ar-*H*), 8.02 ppm (2H, d, *J* = 8.52 Hz, Ar-*H*), 7.62 ppm (2H, ddd, *J* = 7.68, 7.68, 1.24 Hz, Ar-*H*), 7.53 ppm (2H, ddd, *J* = 7.56, 7.56, 0.96 Hz, Ar-*H*), 4.15 ppm (1H, s, carborane_C-*H*), and 3.50–1.53 ppm (10H, br, B-*H*). ^{13}C NMR (100 MHz, $CDCl_3$, Figure S2): δ 133.7 ppm, 130.9 ppm, 130.0 ppm, 129.0 ppm, 127.7 ppm, 126.0 ppm, 125.7 ppm, 113.1 ppm, 93.9 ppm, and 63.4 ppm. ^{11}B NMR (128 MHz, $CDCl_3$ Figure S3): δ: −1.4 ppm, −2.6 ppm, −4.3 ppm, −8.3 ppm, −9.5 ppm, −10.5 ppm, and −12.2 ppm, −13.6. HRMS (APCI): calculated for $C_{18}H_{20}B_{10}$ $[M + Cl]^-$ *m/z* 381.2190, found *m/z* 381.2197.

Synthesis of dCBEA

A mixture of 9,10-diiodoanthracene (0.2170 g, 0.504 mmol), CuI (0.0773 g, 0.406 mmol), $Pd_2(dba)_3$ (0.0467 g, 0.0510 mmol), and TFP (0.0584 g, 0.252 mmol) was dissolved in 20 mL of THF and 10 mL of triethylamine under an Ar atmosphere.

Table 3. Optical properties of the O-form crystal and after various treatments

condition	λ_{PL} (nm)[a]	Color coordination (x, y)[b]	τ (ns)[c]	Φ_{PL}[d]
Pristine	575	(0.48, 0.52)	2.27 (77%) 4.13 (23%)	0.02
Smashed	560	(0.37, 0.62)	2.16 (71%) 3.83 (29%)	0.03
Ground	543	(0.25, 0.74)	4.41 (34%) 15.0 (66%)	0.07
Heated	557	(0.35, 0.65)	1.73 (65%) 3.36 (35%)	0.03
Fumed	560	(0.37, 0.62)	2.08 (69%) 3.68 (31%)	0.03

[a]Excited at 400 nm.
[b]Estimated from the CIE diagram according to λ_{PL}.
[c]We calculated the decay curve with the excitation light at 375, nm as shown in Figure S11.
[d]Determined as an absolute value.

1-Ethynyl*o*-carborane (0.1688 g, 1.00 mmol) was added, and the mixture was stirred at room temperature for 20 h in the dark. The reaction mixture was washed with NH_4Cl, and the organic layer was dried over $MgSO_4$. After $MgSO_4$ was removed, the solvent was evaporated. The residue was purified by column chromatography on silica gel (hexane/THF, v/v = 7:1). After evaporation of the solvent, recrystallization from $CHCl_3$/MeOH afforded compound **dCBEA** as a yellow solid (0.1665 g, 0.326 mmol, 65%). ^{1}H NMR (400 MHz, $CDCl_3$, Figure S4): δ 8.30 ppm (4H, dd, Ar-*H*), 7.68 ppm (4H, dd, Ar-*H*), 4.14 ppm (2H, s, carborane_C-*H*), and 3.70–1.60 ppm (20H, br, B-*H*). ^{13}C NMR (100 MHz, $CDCl_3$, Figure S5): δ 132.7 ppm, 128.1 ppm, 126.4 ppm, 116.5 ppm, 95.9 ppm, 77.2 ppm, 75.6 ppm, and 63.1 ppm. ^{11}B NMR (128 MHz, $CDCl_3$, Figure S6): δ −1.3 ppm, −2.5 ppm, −8.1 ppm, −9.3 ppm, −10.5 ppm, and −13.3 ppm. HRMS (APCI): Calculated for $C_{22}H_{30}B_{20}$ $[M + Cl]^-$ *m/z* 549.3951, found *m/z* 549.3946.

Synthesis of dCBEP

A mixture of 1,6-diiodopyrene (0.0543 g, 0.119 mmol), CuI (0.0185 g, 0.0971 mmol), $Pd_2(dba)_3$ (0.0114 g, 0.0124 mmol), and TFP (0.0139 g, 0.0599 mmol) was dissolved

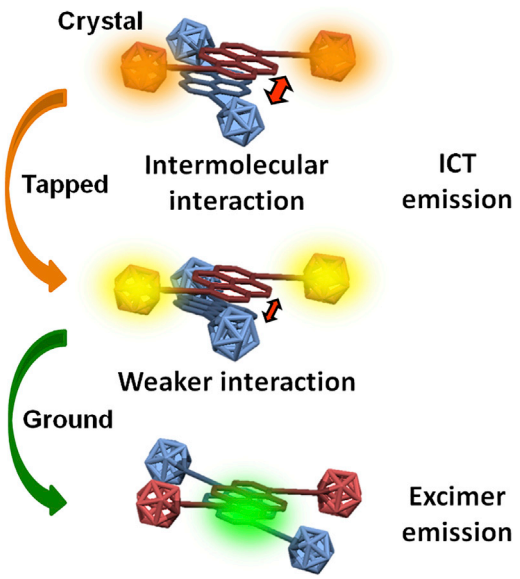

Figure 8. Plausible luminescence model
Shown is a plausible model of multi-step mechanochromic luminescence, including the switching process from ICT to excimer emission.

in 5 mL of THF and 4 mL of triethylamine under an Ar atmosphere. 1-Ethynylo-carborane (0.0405 g, 0.241 mmol) was added, and the mixture was stirred at 60°C for 1 day. The reaction mixture was washed with NH_4Cl, and the organic layer was dried over $MgSO_4$. After $MgSO_4$ was removed, the solvent was evaporated. The residue was purified by column chromatography on silica gel (hexane/THF, v/v = 4:1). After evaporation of the solvent, recrystallization from toluene afforded compound **dCBEP** as an orange solid (0.0239 g, 0.0447 mmol, 37%). ^{1}H NMR (400 MHz, C_4D_8O, Figure S7): δ 8.45 ppm (2H, d, J = 9.04 Hz, Ar-*H*), 8.31 ppm (2H, d, J = 8.08 Hz, Ar-*H*), 8.29 ppm (2H, d, J = 9.04 Hz, Ar-*H*), 8.21 ppm (2H, d, J = 8.08 Hz, Ar-*H*), 5.24 ppm (2H, s, carborane_C-*H*), and 3.34–1.78 ppm (20H, br, B-*H*). ^{13}C NMR (100 MHz, C_4D_8O, Figure S8): δ 133.6 ppm, 133.0 ppm, 131.6 ppm, 129.8 ppm, 126.7 ppm, 126.6 ppm, 124.3 ppm, 115.9 ppm, 89.8 ppm, 78.5 ppm, 65.2 ppm, and 62.6 ppm. ^{11}B NMR (128 MHz, C_4D_8O, Figure S9): δ −1.8 ppm, −2.9 ppm, −8.3 ppm, −9.5 ppm, and−10.4 ppm. HRMS (APCI): calculated for $C_{24}H_{30}B_{20}$ $[M + Cl]^-$ m/z 573.3946, found m/z 573.3947

SUPPLEMENTAL INFORMATION

Supplemental information can be found online at https://doi.org/10.1016/j.xcrp.2022.100758.

ACKNOWLEDGMENTS

This work was partially supported by the Nakatani Foundation (to K.T.) and JSPS KAKENHI grants JP21H02001 and JP21K19002 (to K.T.).

AUTHOR CONTRIBUTIONS

H.Y., K.T., and Y.C. conceived the research idea. H.Y. and J.O. optimized the experiments and wrote the draft. H.Y. and J.O. carried out the DFT calculation. H.Y., J.O., and K.Y. collected the data. K.T. and H.Y. analyzed the data. All of the authors contributed to the writing paper.

DECLARATION OF INTERESTS

The authors declare no competing interests.

Received: September 29, 2021
Revised: December 22, 2021
Accepted: January 13, 2022
Published: February 2, 2022

REFERENCES

1. Bregadze, V.I. (1992). Dicarba-closo-dodecaboranes $C_2B_{10}H_{12}$ and their derivatives. Chem. Rev. *92*, 209–223.

2. Scholz, M., and Hey-Hawkins, E. (2011). Carbaboranes as pharmacophores: properties, synthesis, and application strategies. Chem. Rev. *111*, 7035–7062.

3. Núñez, R., Terrés, M., Ferrer-Ugalde, A., Biani, F.F.d., and Teixidor, F. (2016). Electrochemistry and photoluminescence of icosahedral carboranes, boranes, metallacarboranes, and their derivatives. Chem. Rev. *116*, 14307–14378.

4. Issa, F., Kassiou, M., and Rendina, L.M. (2011). Boron in drug discovery: carboranes as unique pharmacophores in biologically active compounds. Chem. Rev. *111*, 5701–5722.

5. Núñez, R., Romero, I., Teixidor, F., and Viñas, C. (2016). Icosahedral boron clusters: a perfect tool for the enhancement of polymer features. Chem. Soc. Rev. *45*, 5147.

6. Shan, H., Liu, A., Lv, Y., Wu, X., Ma, Y., Jin, X., and Guo, J. (2020). Manipulating the AIE and low-temperature phosphorescence properties of o-carborane-imidazole derivatives via fine tuning their structural features. Dyes Pigm. *180*, 108400.

7. Li, X., Zhou, Q., Zhu, M., Chen, W., Wang, B., Sha, Y., and Yan, H. (2021). Color-tunable and highly emissive solid materials constructed from tetraphenylethylene-o-carborane-based building blocks: synthesis, aggregation-induced emission, and photophysics. Chem. Asian J. *16*, 757–760.

8. Mun, M.S., Ryu, C.H., So, H., Kim, M., Lee, J.H., Hwang, H., and Lee, K.M. (2020). Multiple photoluminescence of spiro[acridine-fluorene]-based o-carboranyl compounds with potential as a visual sensory material. J. Mater. Chem. C *8*, 16896–16906.

9. Shida, N., Owaki, S., Eguchi, H., Nishikawa, T., Tomita, I., and Inagi, S. (2020). Bis(pentafluorophenyl)-o-carborane and its arylthio derivatives: synthesis, electrochemistry and optical properties. Dalton Trans. *49*, 12985–12989.

10. Wu, X., Guo, J., Lv, Y., Jia, D., Zhao, J., Shan, H., Jin, X., and Ma, Y. (2020). Aggregation-induced emission characteristics of o-carborane-functionalized fluorene and its heteroanalogs: the influence of heteroatoms on

photoluminescence. Mater. Chem. Front. *4*, 257–267.

11. Wang, Z., Zhao, J., Muddassir, M., Guan, R., and Tao, S. (2021). Recovering the thermally activated delayed fluorescence in aggregation-induced emitters of carborane. Inorg. Chem. *60*, 4705–4716.

12. Ochi, J., Tanaka, K., and Chujo, Y. (2020). Recent progresses in the development of solid-state luminescent o-carboranes with stimuli responsivity. Angew. Chem. Int. Ed. *132*, 9841–9855.

13. Li, J., Hou, C., Huang, C., Xu, S., Peng, X., Qi, Q., Lai, W.-Y., and Huang, W. (2020). Boosting circularly polarized luminescence of organic conjugated systems via twisted intramolecular charge transfer. Research *2020*, 3839160.

14. Li, J., Yang, C., Peng, X., Qi, Q., Li, Y., Lai, W.-Y., and Huang, W. (2017). Stimuli-responsive circularly polarized luminescence from an achiral perylenyl dyad. Org. Biomol. Chem. *15*, 8463–8470.

15. Liu, X., Sang, M., Lin, H., Liu, C., Zhang, J., Yi, J., Gao, K., Lai, W.-Y., and Huang, W. (2020). Donor–acceptor type pendant conjugated molecules based on a triazine center with depressed intramolecular charge transfer characteristics as gain media for organic semiconductor lasers. Chem. Eur. J. *26*, 3103–3112.

16. Lee, S., Shin, J., Ko, D.-H., and Han, W.-S. (2020). A new type of carborane-based electron-accepting material. Chem. Commun. *56*, 12741–12744.

17. Wang, Z., Jiang, P., Wang, T., Moxey, G.J., Cifuentes, M.P., Zhang, C., and Humphrey, M.G. (2016). Blue-shifted emission and enhanced quantum efficiency via π-bridge elongation in carbazole–carborane dyads. Phys. Chem. Chem. Phys. *18*, 15719–15726.

18. Kwon, S., Wee, K.-R., Cho, Y.-J., and Kang, S.O. (2014). Carborane dyads for photoinduced electron transfer: photophysical studies on carbazole and phenyl-o-carborane molecular assemblies. Chem. Eur. J. *20*, 5953–5960.

19. Ochi, J., Tanaka, K., and Chujo, Y. (2021). Experimental proofs for emission annihilation through bond elongation at the carbon–carbon bond in o-carborane with fused biphenyl-substituted compounds. Dalton Trans. *50*, 1025–1033.

20. Naito, H., Nishino, K., Morisaki, Y., Tanaka, K., and Chujo, Y. (2017). Solid-state emission of the anthracene−o-carborane dyad via twisted-intramolecular charge transfer in the crystalline state. Angew. Chem. Int. Ed. *56*, 254–259.

21. Li, J., Yang, C., Peng, X., Chen, Y., Qi, Q., Luo, X., Lai, W.-Y., and Huang, W. (2018). Stimuli-responsive solid-state emission from o-carborane–tetraphenylethene dyads induced by twisted intramolecular charge transfer in the crystalline state. J. Mater. Chem. C *6*, 19–28.

22. Nishino, K., Tanaka, K., Morisaki, Y., and Chujo, Y. (2019). Design of thermochromic luminescence without conformation and morphology changes by employing the bis(o-carborane)-substituted benzobithiophene structure. Chem. Asian J. *14*, 789–795.

23. Li, J., Hou, C., Qi, Q., Jiao, L., Dai, L., Chen, D., Geng, H., Lai, W.-Y., and Huang, W. (2021). Thermal energy-driven solid-state molecular rotation monitored by real-time emissive color switching. CCS Chem. *3*, 2749–2761.

24. Tanaka, K., and Chujo, Y. (2020). Modulation of the solid-state luminescent properties of conjugated polymers by changing the connecting points of flexible boron element-blocks. Polym. J. *52*, 555–566.

25. Gon, M., Tanaka, K., and Chujo, Y. (2019). Concept of excitation-driven boron complexes and their applications for functional luminescent materials. Bull. Chem. Soc. Jpn. *92*, 7–18.

26. Gon, M., Tanaka, K., and Chujo, Y. (2018). Recent progress in the development of advanced element-block materials. Polym. J. *50*, 109–126.

27. Chujo, Y., and Tanaka, K. (2015). New polymeric materials based on element-blocks. Bull. Chem. Soc. Jpn. *88*, 633–643.

28. Nishino, K., Yamamoto, H., Tanaka, K., and Chujo, Y. (2016). Development of solid-state emissive materials based on multi-functional o-carborane-pyrene dyads. Org. Lett. *18*, 4064–4067.

29. Naito, H., Nishino, K., Morisaki, Y., Tanaka, K., and Chujo, Y. (2017). Luminescence color tuning of stable luminescent solid materials from blue to NIR based on bis-o-carborane-substituted oligoacenes. Chem. Asian J. *12*, 2134–2138.

30. Nishino, K., Uemura, K., Tanaka, K., and Chujo, Y. (2017). Enhancement of aggregation-induced emission by introducing multiple o-carborane substitutions into triphenylamine. Molecules *22*, 2009–2018.

31. Naito, H., Nishino, K., Morisaki, Y., Tanaka, K., and Chujo, Y. (2017). Highly-efficient solid-state emissions of the anthracene−o-carborane dyads with various substituents and their thermochromic luminescent properties. J. Mater. Chem. C *4*, 10047–10054.

32. Naito, H., Uemura, K., Morisaki, Y., Tanaka, K., and Chujo, Y. (2018). Enhancement of luminescence efficiencies by thermal rearrangement from ortho- to meta-carborane in bis-carborane-substituted acenes. Eur. J. Org. Chem. *2018*, 1885–1890.

33. Nishino, K., Uemura, K., Tanaka, K., Morisaki, Y., and Chujo, Y. (2018). Modulation of the cis- and trans-conformations in the bis-o-carborane substituted benzodithiophenes and emission enhancement effect on luminescent efficiency by solidification. Eur. J. Org. Chem. *2018*, 1507–1512.

34. Wada, K., Hashimoto, K., Ochi, J., Tanaka, K., and Chujo, Y. (2021). Rational design for thermochromic luminescence in amorphous polystyrene films with the bis-o-carborane-substituted enhanced-conjugated molecule having aggregation-induced luminochromism. Aggregate *2*, e93.

35. Nishino, K., Hashimoto, K., Tanaka, K., Morisaki, Y., and Chujo, Y. (2018). Comparison of luminescent properties of helicene-like bibenzothiophenes with o-carborane and 5,6-dicarba-nido-decaborane. Sci. China Chem. *61*, 940–946.

36. Mori, H., Nishino, K., Wada, K., Morisaki, Y., Tanaka, K., and Chujo, Y. (2018). Modulation of luminescent chromic behaviors and environment-responsive intensity changes by substituents in bis-o-carborane-substituted conjugated molecules. Mater. Chem. Front. *2*, 573–579.

37. Nishino, K., Tanaka, K., and Chujo, Y. (2019). Tuning of sensitivity in thermochromic luminescence by regulating molecular rotation based on triphenylamine-substituted o-carboranes. Asian J. Org. Chem. *8*, 2228–2232.

38. Marsh, A.V., Cheetham, N.J., Little, M., Dyson, M., White, A.J.P., Beavis, P., Warriner, C.N., Swain, A.C., Stavrinou, P.N., and Heeney, M. (2018). Carborane-induced excimer emission of severely twisted bis-*o*-carboranyl chrysene. Angew. Chem. Int. Ed. *57*, 10640–10645.

39. Ochi, J., Tanaka, K., and Chujo, Y. (2019). Improvement of solid-state excimer emission of the aryl−ethynyl−o-carborane skeleton by acridine introduction. Eur. J. Org. Chem. *2019*, 2984–2988.

40. Ochi, J., Tanaka, K., and Chujo, Y. (2021). Dimerization-induced solid-state excimer emission showing consecutive thermochromic luminescence based on acridine-modified o-carboranes. Inorg. Chem. *60*, 8990–8997.

41. Nishino, K., Yamamoto, H., Tanaka, K., and Chujo, Y. (2017). Solid-state themochromic luminescence via twisted intramolecular charge transfer and excimer formation of the carborane-pyrene dyad with an ethynyl spacer. Asian J. Org. Chem. *6*, 1818–1822.

42. Nishino, K., Yamamoto, H., Tanaka, K., and Chujo, Y. (2019). Time-dependent emission enhancement of the etynylpyrene-o-carborane dyad and its application as a luminescent color sensor for evaluating water contents in organic solvents. Chem. Asian J. *14*, 1577–1581.

43. Wu, X., Guo, J., Quan, Y., Jia, W., Jia, D., Chen, Y., and Xie, Z. (2018). Cage carbon-substitute does matter for aggregation-induced emission features of o-carborane-functionalized anthracene triads. J. Mater. Chem. C *6*, 4140–4149.

44. Zhang, Z., Zhang, Y., Yao, D., Bi, H., Javed, I., Fan, Y., Zhang, H., and Wang, Y. (2009). Anthracene-arrangement-dependent emissions of crystals of 9-anthrylpyrazole derivatives. Cryst. Growth Des. *9*, 5069–5072.

45. Iida, A., and Yamaguchi, S. (2009). Intense solid-state blue emission with a small Stokes' shift: π-stacking protection of the diphenylanthracene skeleton. Chem. Commun. *21*, 3002–3004.

46. Fujiwara, Y., Ozawa, R., Onuma, D., Suzuki, K., Yoza, K., and Kobayashi, K. (2013). Double alkylene-strapped diphenylanthracene as a

photostable and intense solid-state blue-emitting material. J. Org. Chem. *78*, 2206–2212.

47. Percino, J., Cerón, M., Venkatesan, P., Ceballos, P., Bañuelos, A., Rodríguez, O., Siegler, M.A., Robles, F., Chapela, V.M., Soriano-Moro, G., et al. (2017). Two different emissions of (2Z)-2-(4-bromophenyl)-3-[4-(dimethylamino) phenyl]prop-2-enenitrile due to crystal habit and size: synthesis, optical, and supramolecular characterization. Cryst. Growth Des. *17*, 1679–1694.

48. Wang, L., Wank, K., Zou, B., Ye, K., Zhang, H., and Wang, Y. (2015). Luminescent chromism of boron diketonate crystals: distinct responses to different stresses. Adv. Mater. *27*, 2918–2922.

49. Lin, Z., Mei, X., Yang, E., Li, X., Yao, H., Wen, G., Chien, C.-T., Chow, T.J., and Ling, Q. (2014). Polymorphism-dependent fluorescence of bisthienylmaleimide with different responses to mechanical crushing and grinding pressure. CrystEngComm. *16*, 11018–11026.

50. Ito, S., Yamada, T., and Asami, M. (2016). Two-step mechanochromic luminescence of N,N′-bis-Boc-3,3′-di(pyren-1-yl)-2,2′-biindole. ChemPlusChem. *81*, 1272–1275.

51. Saotome, S., Suenaga, K., Tanaka, K., and Chujo, Y. (2020). Design for multi-step mechanochromic luminescence property by enhancement of environmental sensitivity in a solid-state emissive boron complex. Mater. Chem. Front. *4*, 1781–1788.

52. Guo, J., Liu, D., Zhang, J., Zhang, J., Miao, Q., and Xie, Z. (2015). o-Carborane functionalized pentacenes: synthesis, molecular packing and ambipolar organic thin-film transistors. Chem. Commun. *51*, 12004–12007.

53. Shao, M., Dongare, P., Dawe, L.N., Thompson, D.W., and Zhao, Y. (2010). Biscrown-annulated TTFAQ−Dianthracene hybrid: synthesis, structure, and metal ion sensing. Org. Lett. *12*, 3050–3053.

54. Lübtow, M., Helmers, I., Stepanenko, V., Albuquerque, R.Q., Marder, T.B., and Fernández, G. (2017). Self-assembly of 9,10-Bis(phenylethynyl) anthracene (BPEA) derivatives: influence of π–π and hydrogen-bonding interactions on aggregate morphology and self-assembly mechanism. Chem. Eur. J. *23*, 6198–6205.

55. Abe, H., Mawatari, Y., Teraoka, H., Fujimoto, K., and Inouye, M. (2004). Synthesis and molecular recognition of pyrenophanes with Polycationic or amphiphilic functionalities:artificial plate -shapedcavitant incorporating arenes and nucleotides in water. J. Org. Chem. *69*, 495–504.